

Cell Reports, Volume 24

Supplemental Information

Adaptive Evolution of MERS-CoV

to Species Variation in DPP4

Michael Letko, Kerri Miazgowicz, Rebekah McMinn, Stephanie N. Seifert, Isabel Sola, Luis Enjuanes, Aaron Carmody, Neeltje van Doremalen, and Vincent Munster

Supplemental figures.

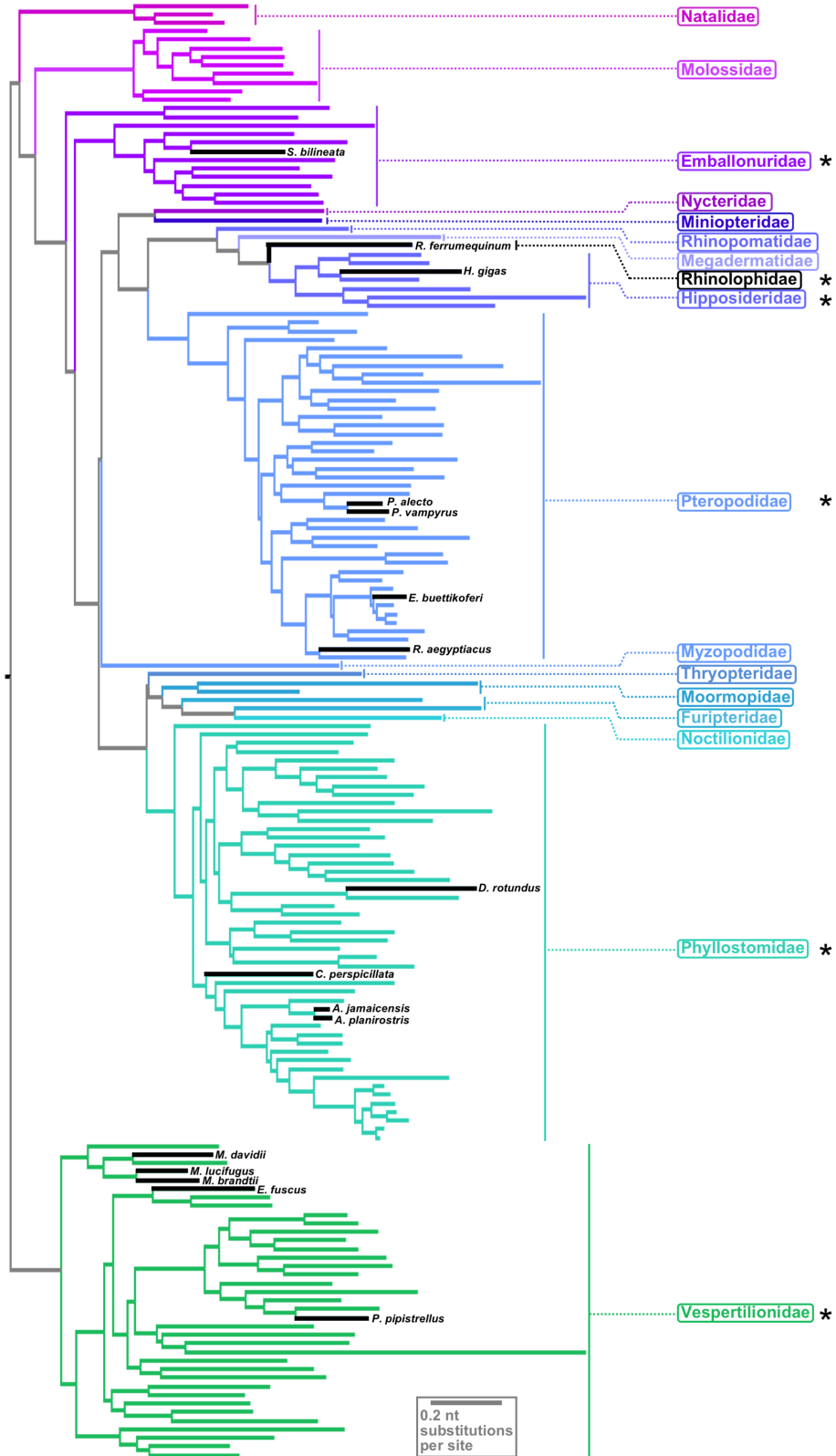


Figure S1. Phylogenetic relationship of bat species from this study. *Related to Figure 1.* Bat phylogenetic relationships were reconstructed for the 166 genera and 17 families in the order Chiroptera for which at least one

cytochrome b sequence >1000bp in length was available in the NCBI database (accessed February 2018). A phylogenetic tree was inferred using maximum likelihood estimation with a general time-reversible model of sequence evolution and estimated values of the proportion of invariable sites and rate variation among sites (GTR+G+I) implemented in PhyML 3.0 (Guindon et al., 2010). The model of sequence evolution was selected by Bayesian Information Criterion in SMS v1.8.1 (Lefort et al., 2017). The sixteen bat species selected for this study are indicated in black with species names adjacent to their respective branches and family-level identification to the right of the phylogenetic tree. Scale bar represents nucleotide substitutions per site. Asterisks indicate families represented in this study.

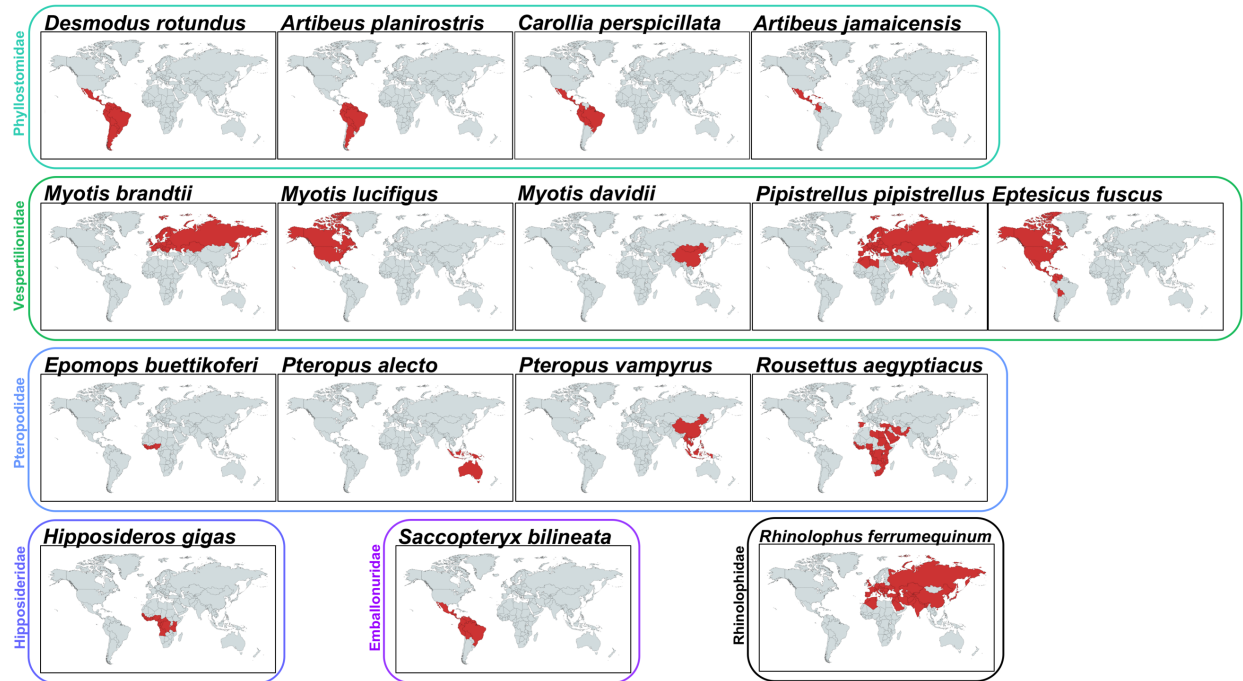


Figure S2. Geographic distribution of bat species from this study. Related to Figure 1. Countries of occurrence for each of the 16 bat species from this study were obtained from The International Union for Conservation of Nature (www.iucnredlist.org) and mapped using MapChart (mapchart.net).

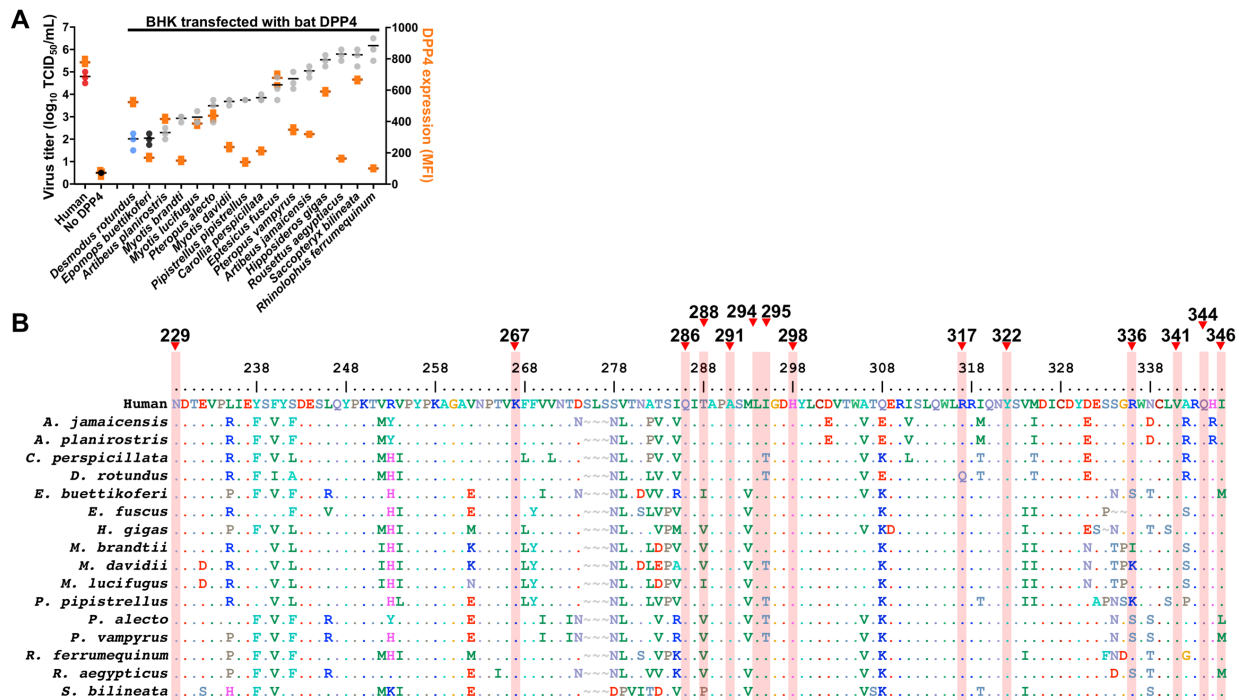


Figure S3. Bat DPP4 surface expression and extended amino acid alignment of DPP4 region that interacts with spike. Related to Figure 1. (A) Surface expression data is overlaid on top of the viral titer data from figure 1B. BHK cells were transfected with equivalent amounts of DPP4 expression plasmids and DPP4 surface expression was measured by flow cytometry 24 hours later. Surface expression data from three replicates is represented as geometric mean fluorescence intensity, depicted in orange boxes. **(B)** Shown are DPP4 residues 229-346 (human numbering), which encompass the 14 described spike-contact points described in Wang et al. 2013 (highlighted in red with numbers indicated above).

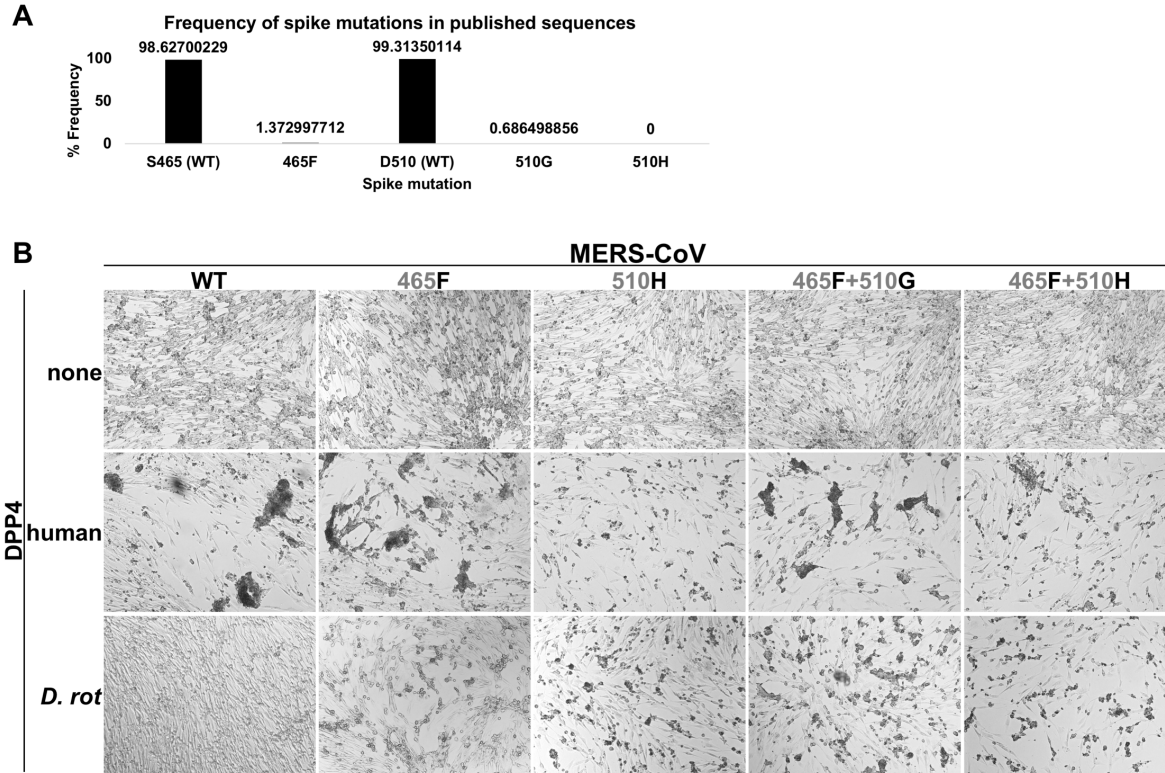


Figure S4. Frequency of spike mutants in published sequences and microscopy of reverse genetics viruses. Related to Figure 2 and Figure 3. (A) Four hundred thirty seven MERS spike amino acid sequences were downloaded from PubMed and analyzed for the presence of mutations at residues 465 and 510. (B) Point mutations were introduced into the spike coding sequence of the MERS-CoV/EMC12 genome. Transduced BHK cell lines were infected with mutant viruses at an MOI of 0.001. Standard light microscopy, 20X, shown at 48-hours post-infection.

Supplemental References

Guindon, S., Dufayard, J.F., Lefort, V., Anisimova, M., Hordijk, W., and Gascuel, O. (2010). New algorithms and methods to estimate maximum-likelihood phylogenies: assessing the performance of PhyML 3.0. *Syst Biol* 59, 307-321.

Lefort, V., Longueville, J.E., and Gascuel, O. (2017). SMS: Smart Model Selection in PhyML. *Mol Biol Evol* 34, 2422-2424.